**Tianjin Daxue Xuebao (Ziran Kexue yu Gongcheng Jishu Ban)/**
**Journal of Tianjin University Science and Technology**
ISSN (Online):0493-2137
E-Publication: Online Open Access
Vol: 55 Issue: 12:2022
DOI: 10.5281/zenodo.19247821

# EXPERIMENTAL ANALYSIS OF CHARACTERIZATION OF IMPACT ZONES IN AA2024 / AA7075 WELDED JOINTS OF FRICTION STIR

**Dr. SURESH JADHAV***
Assistant Professor, Department of Mechanical Engineering VJTI Matunga, Mumbai, India. * Corresponding Author Email: sgjadhav@me.vjti.ac.in

**SIDDHESH JAITAPKAR**
Department of Mechanical Engineering VJTI Matunga, Mumbai, India.

**Dr. SUNIL BHAMARE**
Joint Director, Directorate of Technical Education Mumbai, India.

**Abstract**

Friction Stir Welding (FSW) is an advanced solid-state joining technique that utilizes a rotating tool to generate frictional heat, facilitating plastic deformation for material consolidation. This process ensures defect-free joints while maintaining structural integrity, making it a preferable alternative to conventional fusion welding, especially for aluminum alloys with poor weldability. In this study, the microstructural characteristics of FSW joints in homogeneous and heterogeneous aluminum alloys (AA2024 and AA7075) are analyzed. The mechanical properties of the weld are influenced by the base materials at the advancing side (AS) and retreating side (RS). Microstructural evaluation reveals particle coarsening in critical regions, including the thermo-mechanically affected zone, nugget zone, and heat-affected zone. Variations in chemical constituents result in different peak intensities due to crystallographic changes. These effects are observed across the heat-affected zone, thermo-mechanically affected zone, and base material regions on both the advancing and retreating sides in dissimilar FSW joints. The findings contribute to a deeper understanding of microstructural evolution in FSW, aiding in process optimization for enhanced joint performance.

## INTRODUCTION

Friction Stir Welding (FSW) was first developed in 1991 by The Welding Institute (TWI) in the United Kingdom's [1]. Unlike conventional welding techniques, FSW enables material fusion without reaching its melting point, making it highly effective for welding non-ferrous metals, particularly aluminum alloys. These alloys pose challenges in conventional welding due to their sensitivity to heat and mechanical property degradation. Over time, Mishra and his team expanded FSW applications, further advancing the technique [2]. The welding of heterogeneous aluminum alloys presents significant difficulties due to variations in their metallurgical, chemical, and mechanical characteristics. AA2024 and AA7075 are widely used in aerospace applications, particularly in structural components, necessitating the development of reliable and high-strength joints. Traditional fusion welding methods often fail to provide adequate bonding strength due to excessive heat input, which can negatively affect material properties, especially in heat-treated aluminum alloys such as those in the 2xxx and 7xxx series [3]. FSW leads to distinct microstructural changes that categorize the weld into four zones: Base Material (BM), Heat-Affected Zone (HAZ), Thermo-Mechanically Affected Zone (TMAZ), and Nugget Zone (NZ). The BM remains unaffected, while the HAZ undergoes thermal exposure without plastic

**Tianjin Daxue Xuebao (Ziran Kexue yu Gongcheng Jishu Ban)/**
**Journal of Tianjin University Science and Technology**
ISSN (Online):0493-2137
E-Publication: Online Open Access
Vol: 55 Issue: 12:2022
DOI: 10.5281/zenodo.19247821

deformation. The TMAZ experiences both heat and plastic deformation, resulting in structural changes but insufficient strain for complete recrystallization. The NZ, subjected to intense plastic deformation and high temperatures, undergoes dynamic recrystallization, sometimes forming an onion-ring pattern. Fractures in FSW aluminum joints typically occur at the TMAZ-NZ interface due to microstructural inconsistencies [4].

Several studies have analyzed the influence of welding conditions on the microstructural evolution and mechanical performance of AA2024/AA7075 FSW joints. Zhang et al. (2020) determined that microstructural evolution within the stir zone (SZ) is primarily affected by heat input and material flow, leading to refined grain structures and intermetallic compound formation [5]. Similarly, El-Sayed et al. (2021) investigated the role of tool geometry, welding speed, and post-weld treatments, demonstrating their impact on joint integrity [6]. Additionally, Sharifitabar and Nami (2011) explored interfacial bonding mechanisms, emphasizing the role of reinforcing particles in enhancing weld strength [7]. The link between control factors and mechanical performance has been widely studied. Riaz et al. (2021) demonstrated that tool rotational speed is a critical factor in controlling grain refinement and tensile properties [8]. Furthermore, Amancio-Filho et al. (2008) highlighted how intermetallic phases influence mechanical performance [9]. Computational approaches have also been employed to understand FSW dynamics, with Asadi et al. (2016) simulating dynamic recrystallization behavior [10] and Iqbal et al. (2020) developing predictive models for microstructural formation [11]. Research has also focused on microstructural defects, grain growth, and phase transformations. Flores et al. (n.d.) studied the formation of grain structures and defects in welded joints [12]. Fuller et al. (2010) examined post-weld aging effects, showing its influence on hardness and tensile strength [13]. Liu et al. (2008) further investigated intermetallic phase formation at weld interfaces, revealing complex metallurgical interactions that affect joint quality [14].

These studies highlight the critical role of process optimization, microstructural analysis, and computational modeling in improving AA2024/AA7075 FSW joints. Continued advancements in tool design, heat management, and numerical simulation are essential to further refine FSW for dissimilar aluminum alloys.

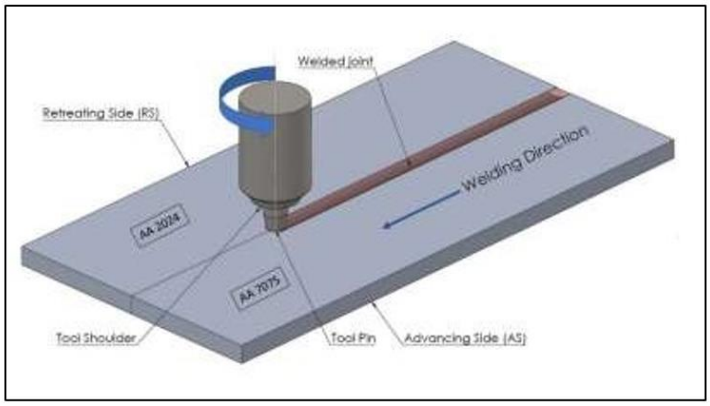


**Figure 1: A visual depiction of the FSW process**

**Tianjin Daxue Xuebao (Ziran Kexue yu Gongcheng Jishu Ban)/**
**Journal of Tianjin University Science and Technology**
ISSN (Online):0493-2137
E-Publication: Online Open Access
Vol: 55 Issue: 12:2022
DOI: 10.5281/zenodo.19247821


**Figure 2: Illustrative map of FSW joint zones [2]**

FSW has garnered increasing attention globally as a sustainable welding technology due to its minimal environmental impact. Unlike fusion welding, which can introduce defects such as voids and cracks, FSW produces superior mechanical properties. Despite extensive research on aluminum alloy microstructures from 1991 to 2017, further investigation is needed to enhance the understanding of joint properties across different welding techniques, including similar, dissimilar, and overlapping FSW approaches. This study aims to analyze the microstructural evolution in FSW joints of AA2024 and AA7075 across different affected zones using various characterization techniques such as OM, SEM, EDS, and XRD.

## 2. EXPERIMENTAL METHODOLOGY

This study used aluminum alloys AA2024-T351 and AA7075-T6, each with a thickness of 4mm and dimensions of 150 mm × 50mm. Table 1 shows the chemical constituents of both alloys, which are validated through material testing. Figure 3(i) shows the FSW procedure utilizing an FSW interface machine.

**Table 1: Chemical constituents of Al alloys (Wt. Percentage)**

| | S | Mn | Si | Cu | Fe | Ti | Mg | Zn | Cr | Al |
|---|---|---|---|---|---|---|---|---|---|---|
| AA7075 - T6 | 0.038 | 0.032 | - | 1.34 | 0.22 | 0.054 | 2.62 | 5.78 | 0.22 | Balance |
| AA2024 - T351 | - | 0.56 | 0.11 | 3.85 | 0.24 | 0.10 | 1.53 | 0.09 | 0.07 | Balance |

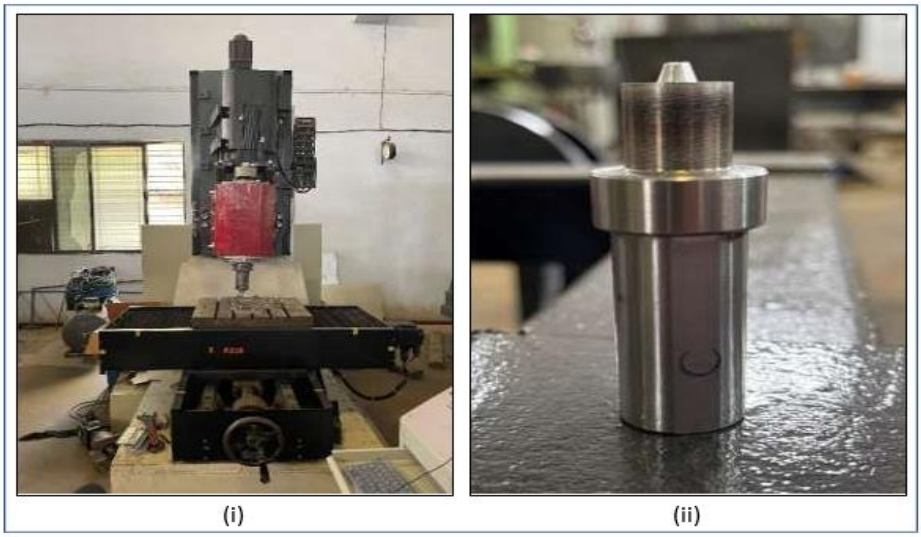


**Figure 3: (i) FSW machine (ii) FSW H13 Tool**

**Tianjin Daxue Xuebao (Ziran Kexue yu Gongcheng Jishu Ban)/**
**Journal of Tianjin University Science and Technology**
ISSN (Online):0493-2137
E-Publication: Online Open Access
Vol: 55 Issue: 12:2022
DOI: 10.5281/zenodo.19247821

The FSW machine operated with a spindle power of 15 kW and an axis motor power of 1 kW, utilizing a clamped butt weld configuration. For both homogeneous and heterogeneous welding, AA2024 and AA7075 were secured on the advancing side and retreating side. The joining process employed an H13 FSW tool, as shown in Figure 3(ii), featuring a hardened surface for enhanced durability. H13, a hot work tool steel, was chosen for its excellent ability to withstand thermal fluctuations, erosion, and wear. The tool was designed with a 3.5 mm-long taper pin, an inward angle of 5°, and a 15 mm shoulder diameter. During the FSW process, the tool rotated in a clockwise direction. For similar material welding of AA2024 and AA7075, the rotational speed was maintained at 700 RPM with a welding speed of 70 mm per min. For heterogenous FSW joints, the rotational speed remained the same at 700 RPM, but the welding speed was reduced to 40 mm per min. The shoulder plunge depth during the welding process was set to 0.2mm.

**Table 2: Keller's Reagent Constituents [6]**

| Ingredients | Volume (ml) |
|---|---|
| Nitric Acid ($HNO_3$) | 05 |
| Hydrochloric Acid (HCl) | 03 |
| Hydrofluoric Acid (HF) | 02 |
| Distilled water | 190 |

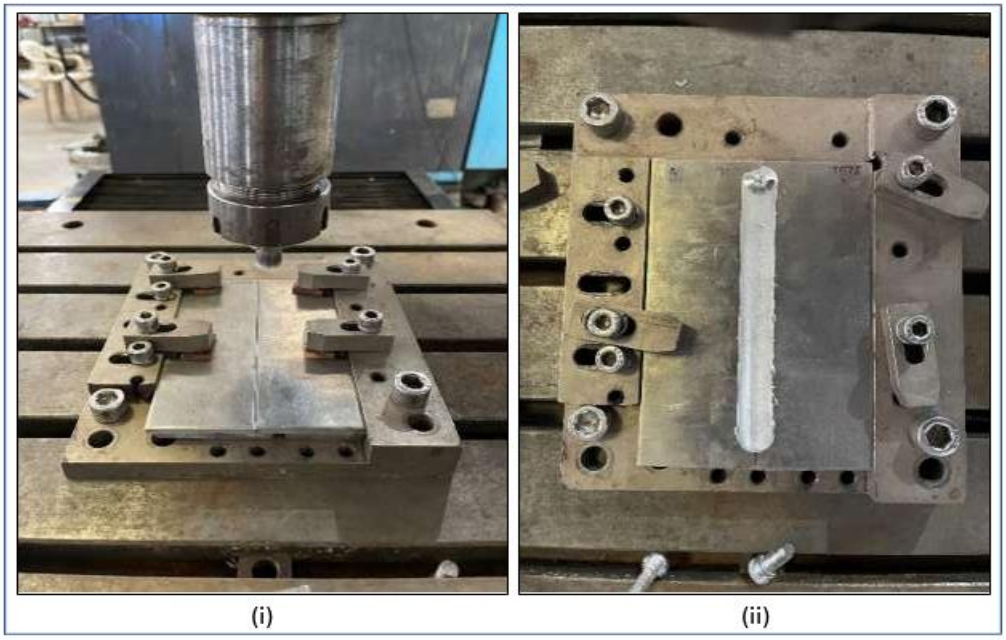


**Figure 4: (i) Material clamped for FSW process (ii) FSW welded joint**

For microstructural analysis, the welded joints were sectioned transversely, at a right angle to the welding direction. Initially, a grinding process was performed to achieve a mirror- like finish on the specimen. Sequential grinding was carried out using abrasive mesh papers of grades 60, 120, 320, 600, 1200, and 2400 to ensure a defect-free

**Tianjin Daxue Xuebao (Ziran Kexue yu Gongcheng Jishu Ban)/**
**Journal of Tianjin University Science and Technology**
ISSN (Online):0493-2137
E-Publication: Online Open Access
Vol: 55 Issue: 12:2022
DOI: 10.5281/zenodo.19247821

surface. A silicon carbide solution was applied to the abrasive paper to enhance the polishing process, resulting in a smooth finish suitable for microstructural examination. The test piece was then etched with Keller's reagent for 30 seconds, with its chemical composition detailed in Table 2. Optical microscopy (ZEISS) was utilized to capture images of different regions of the aluminum alloy. Additionally, SEM (Gemini SEM 300), equipped with EDS, was employed to obtain high-magnification images and analyze the chemical composition of various affected zones resulting from the FSW process. XRD (PANalytical, Empyrean) was performed to determine the phase constituents of the aluminum alloy, considering material crystallography in the dissimilar welded joint, using Cu radiation.

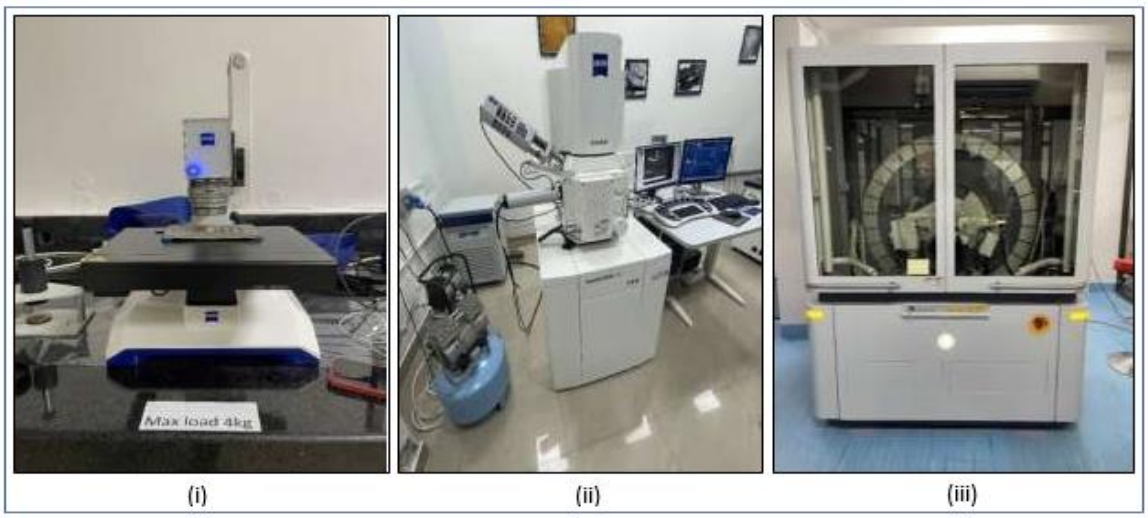


**Figure 5: (i) OM (ii) SEM (iii) XRD**

## 3. RESULT AND DISCUSSION

### 3.1 Microscopic view of the cross-section of welded joints:

The optical micrographs of the base materials (BMs) and nugget zones (NZ) for both AA2024 and AA7075 are presented in Figure 6. In the similar welded joint of AA2024, a cavity is observed in the NZ of the specimen, while the BMs remain unchanged in the optical micrograph. Similarly, for the AA7075 welded joint, the specimen appears over-etched and exhibits signs of corrosion compared to AA2024. A cavity is also present in the NZ of the welded joint. For the dissimilar joint, as shown in Figure, AA2024 appears darker than AA7075 after etching. In the macroscopic view, a basin-shaped structure is visible in the NZ region. The RS- TMAZ exhibits the characteristic onion-ring structure of FSW. Additionally, a crack is observed in the NZ of the specimen. Cavities or cracks serves as indicator of plastic deformation, commonly arising when the tool penetrates the material during welding. On the retreating side, the material's linear velocity is considerably lower than on the AS, influenced by the difference between rotational and welding speeds [1].

**Tianjin Daxue Xuebao (Ziran Kexue yu Gongcheng Jishu Ban)/**
**Journal of Tianjin University Science and Technology**
ISSN (Online):0493-2137
E-Publication: Online Open Access
Vol: 55 Issue: 12:2022
DOI: 10.5281/zenodo.19247821


**Figure 6: Optical microscopy of (i) NZ of AA2024 (ii) BM of AA2024 (iii) NZ of AA7075 (iv) BM of AA7075 (v) NZ of AA2024/7075 (vi) BM of AA2024/7075 (vii) Macroscopic view of AA2024/7075**

### 3.2 Analysis of Phase:

The phases found in the base materials (BMs) and the accompanying thermo, depicted in Figure 7, were investigated using XRD analysis. The XRD patterns reveal various

**Tianjin Daxue Xuebao (Ziran Kexue yu Gongcheng Jishu Ban)/**
**Journal of Tianjin University Science and Technology**
ISSN (Online):0493-2137
E-Publication: Online Open Access
Vol: 55 Issue: 12:2022
DOI: 10.5281/zenodo.19247821

weaker peaks connected to other constituent particles in addition to strong and intense peaks that correspond to the aluminum matrix.

In the AA2024 BM, granule's such as $Al_2Cu$, $Al_2CuMg$, AlCuMg, and $Al_7Cu_2Fe$ are identified, whereas $MgZn_2$ and $Al_7Cu_2Fe$ detected in the AA7075 BM. Moreover, the AS-TMAZ displays lower peak intensity at smaller angles, whereas the $MgZn_2$ peaks in the RS-TMAZ exhibit reduced intensity compered to their respective base materials.

This suggests that these constituent particles undergo dissolution within their respective TMAZ regions. Notably, XRD is limited to detecting phases exceeding 5 wt.%, necessitating the use of EDS analysis for a more detailed identification of precipitated particles [3].

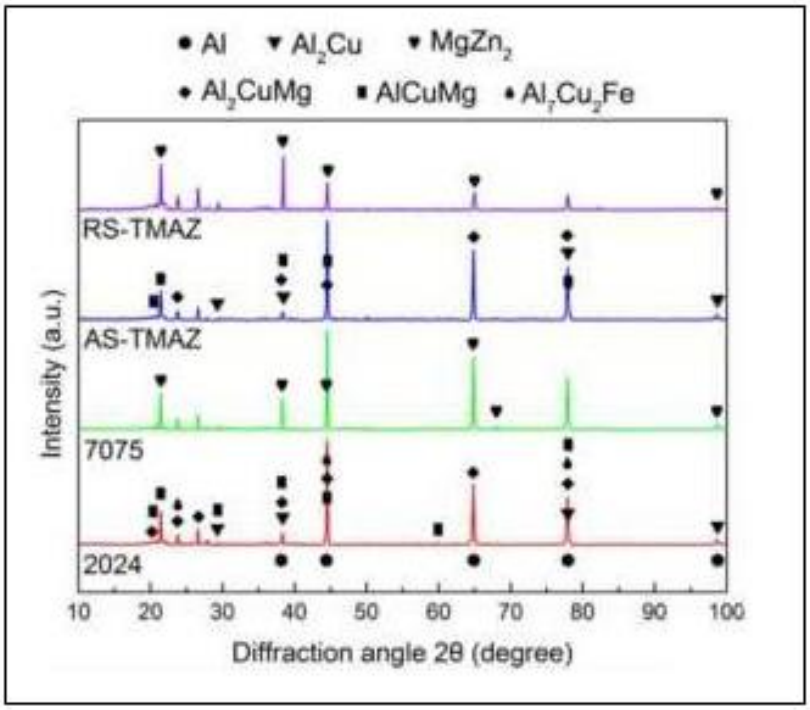


**Figure 7: XRD patterns of dissimilar aluminum alloy weld [3]**

### 3.3 Microstructure and Spectrum Analysis:

Due to the magnification limitations of an optical microscope, it cannot effectively capture the microstructure of a material. Therefore, SEM equipped with EDS is used to analyze both the microstructure and chemical constituents of the affected area. In this study, SEM imaging was performed on homogeneous and heterogeneous welded joints of aluminum alloys, focusing on different zones within the material specimen. For EDS analysis in similar welded joints, no variation in material composition is observed, as both base materials share the same chemical composition. Consequently, there is no significant material mixing in the nugget zone that would alter the chemical constituents and physical properties of the material.

**Tianjin Daxue Xuebao (Ziran Kexue yu Gongcheng Jishu Ban)/**
**Journal of Tianjin University Science and Technology**
ISSN (Online):0493-2137
E-Publication: Online Open Access
Vol: 55 Issue: 12:2022
DOI: 10.5281/zenodo.19247821

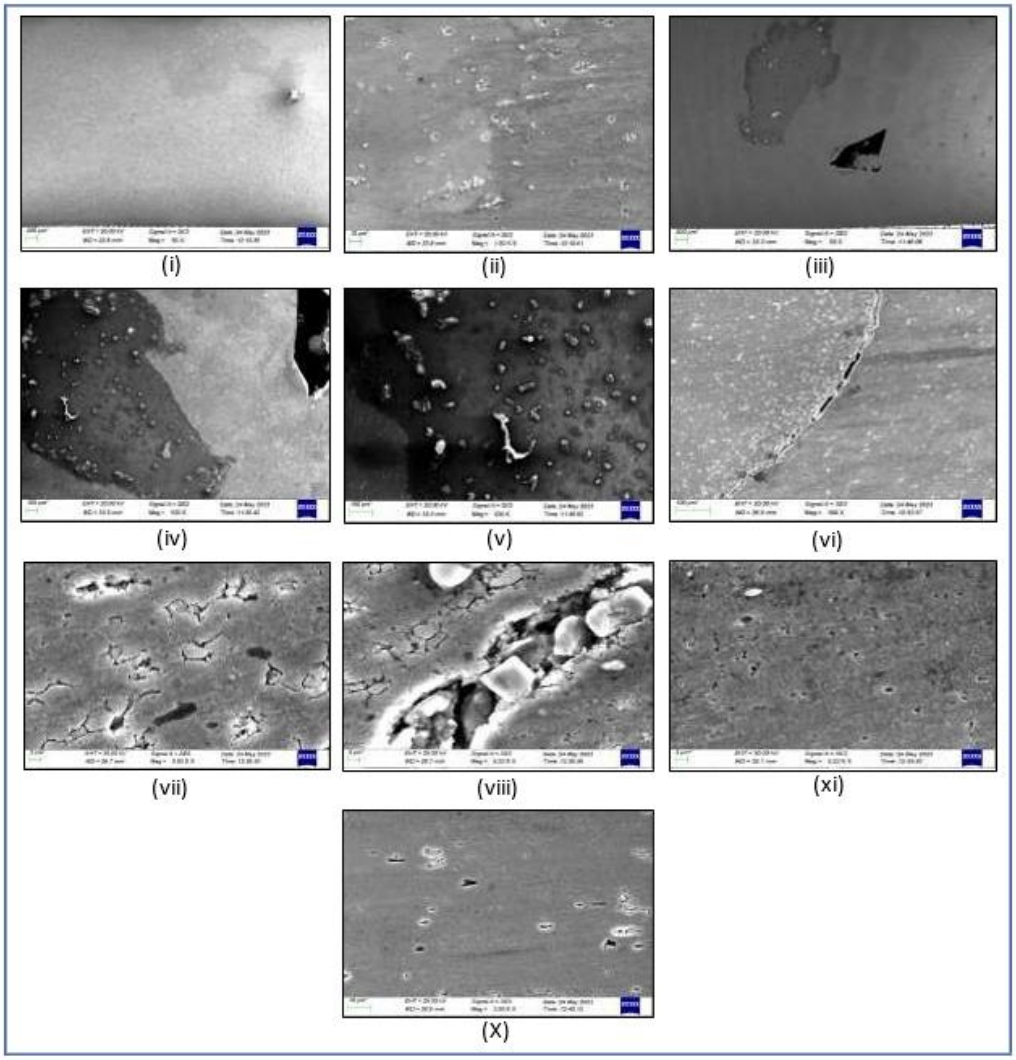


**Figure 8: SEM images (i) NZ of AA2024 (ii) BM of AA2024 (iii) HAZ of AA7075 (iv) TMAZ of AA7075 (v) NZ of AA7075 (vi) NZ of AA2024/7075 (vii) TMAZ of AA2024/7075 (viii) Crack in NZ of AA2024/7075 (ix) BM of AA2024 (x) BM of AA7075**

In this study, SEM analysis reveals the presence of microstructural defects in all specimens of FSW joints, as shown in Figure 8. In the similar weld joint of AA2024, a void is observed along with some grains around the TMAZ. Similarly, in the AA7075 weld joint, a large void, likely caused by the tool tip during welding, is detected near the nugget zone. The NZ appears darker compared to other regions of AA7075. Cracks around the NZ are clearly visible, resulting from the permanent distortion of the material in welding. Additionally, grains are evident in the NZ region of the AA7075 weld. In heterogeneous AA2024/AA7075 weld joint, a prolonged crack appears in the nugget zone, mainly caused by material displacement as the tool penetrates at the welding initiation phase. Plastic deformation around the crack extends to the TMAZ of AA2024. Furthermore, deformed

**Tianjin Daxue Xuebao (Ziran Kexue yu Gongcheng Jishu Ban)/**
**Journal of Tianjin University Science and Technology**
ISSN (Online):0493-2137
E-Publication: Online Open Access
Vol: 55 Issue: 12:2022
DOI: 10.5281/zenodo.19247821

grains are present within the crack in the NZ and along the AS and RS TMAZ regions of the specimen.

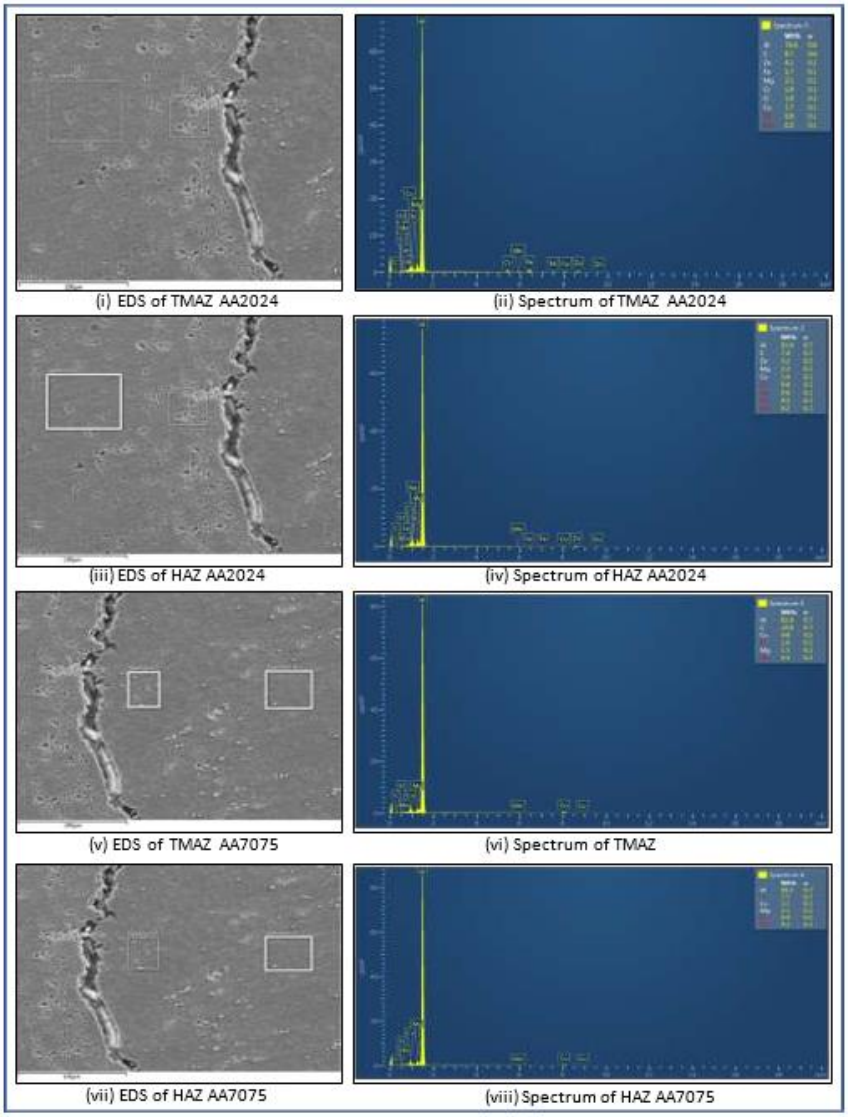


**Figure 9: (i) EDS of TMAZ 2024 (ii) Spectrum of TMAZ 2024 (iii) EDS of HAZ of 2024 (iv) Spectrum of HAZ 2024 (v) EDS of TMAZ 7075 (vi) Spectrum of TMAZ 7075 (vii) EDS of HAZ 7075 (viii) Spectrum of HAZ 7075**

An EDS equipped with SEM is obtained to get the chemical composition in the dissimilar welded joint. As for the similar welded joints no such different material is present after the welding process. In Figure 9 many Zn rich constituents are present in the TMAZ region of 2024 when a spectrum region was analyzed. Further, in the HAZ of 2024 more Zn particles were found due to the mixing of material during welding process. For 7075 spectrum analysis on the TMAZ and HAZ only Cu rich particles were present due to its Advancing side region.

**Tianjin Daxue Xuebao (Ziran Kexue yu Gongcheng Jishu Ban)/**
**Journal of Tianjin University Science and Technology**
ISSN (Online):0493-2137
E-Publication: Online Open Access
Vol: 55 Issue: 12:2022
DOI: 10.5281/zenodo.19247821

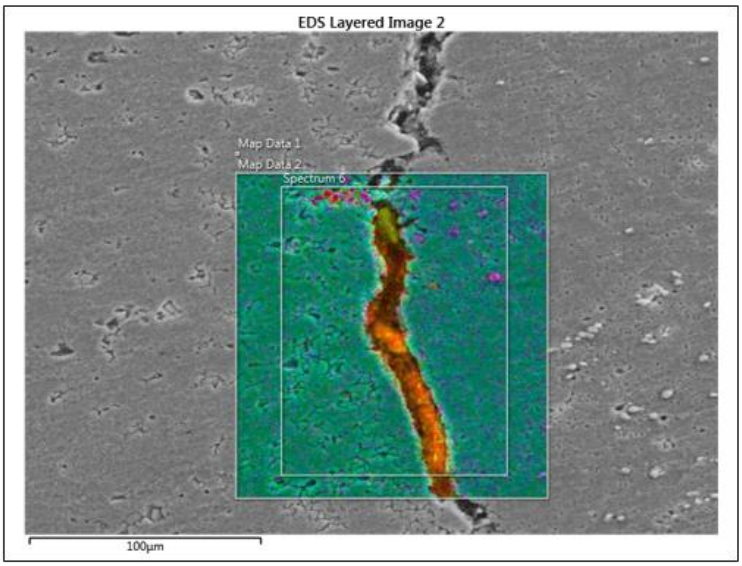


**Figure 10: Element mapping of NZ in 2024/7075**

To visualize the distribution of constituent and concentration of specimen, Element mapping is obtained as seen in Fig 10. Maps of different element in the same area helps determine what phases are present. In this case, mapping of NZ of dissimilar welded joint has been analyzed and the results shown are having elements of Al, Si, Mg, O, Cu and all these are denoted with different color scheme to emphasize on the element on the specific region as illustrated in Figure 11.

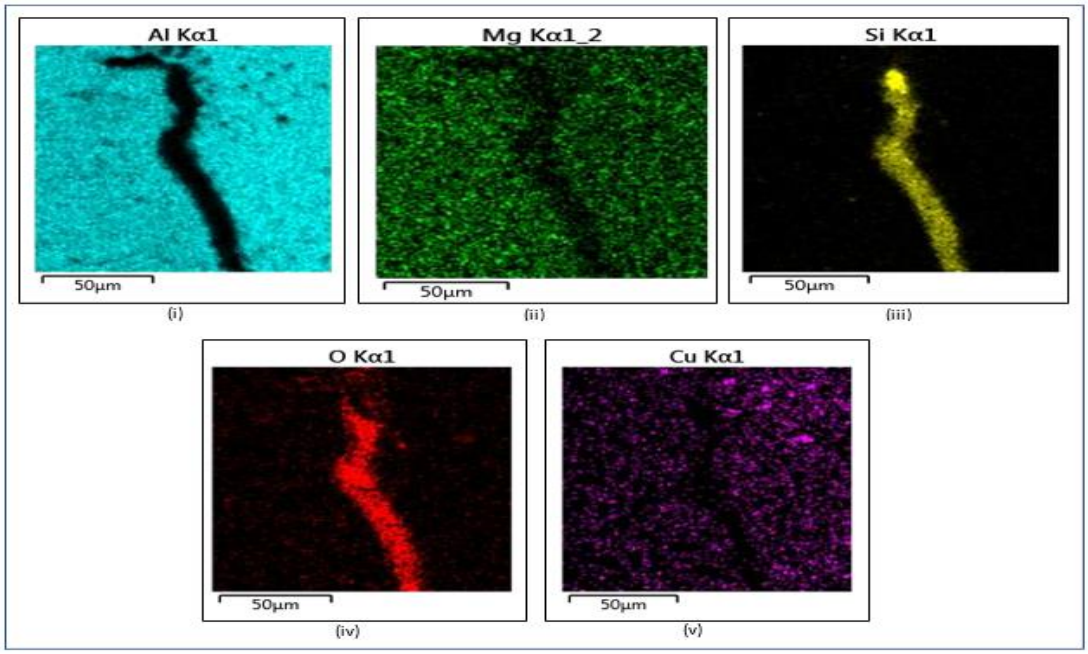


**Figure 11: Element phases of material (i) Al (ii) Mg (iii) Si (iv) O (v) Cu**

**Tianjin Daxue Xuebao (Ziran Kexue yu Gongcheng Jishu Ban)/**
**Journal of Tianjin University Science and Technology**
ISSN (Online):0493-2137
E-Publication: Online Open Access
Vol: 55 Issue: 12:2022
DOI: 10.5281/zenodo.19247821

This study utilized OM, XRD, and SEM/EDS techniques to investigate the micro structural changes and texture development across different regions of the aluminum alloy. For future research, grain size distribution can be examined using EBSD and IPF analysis to identify the grain boundaries and grain size within the NZ resulting from the welding process**.**

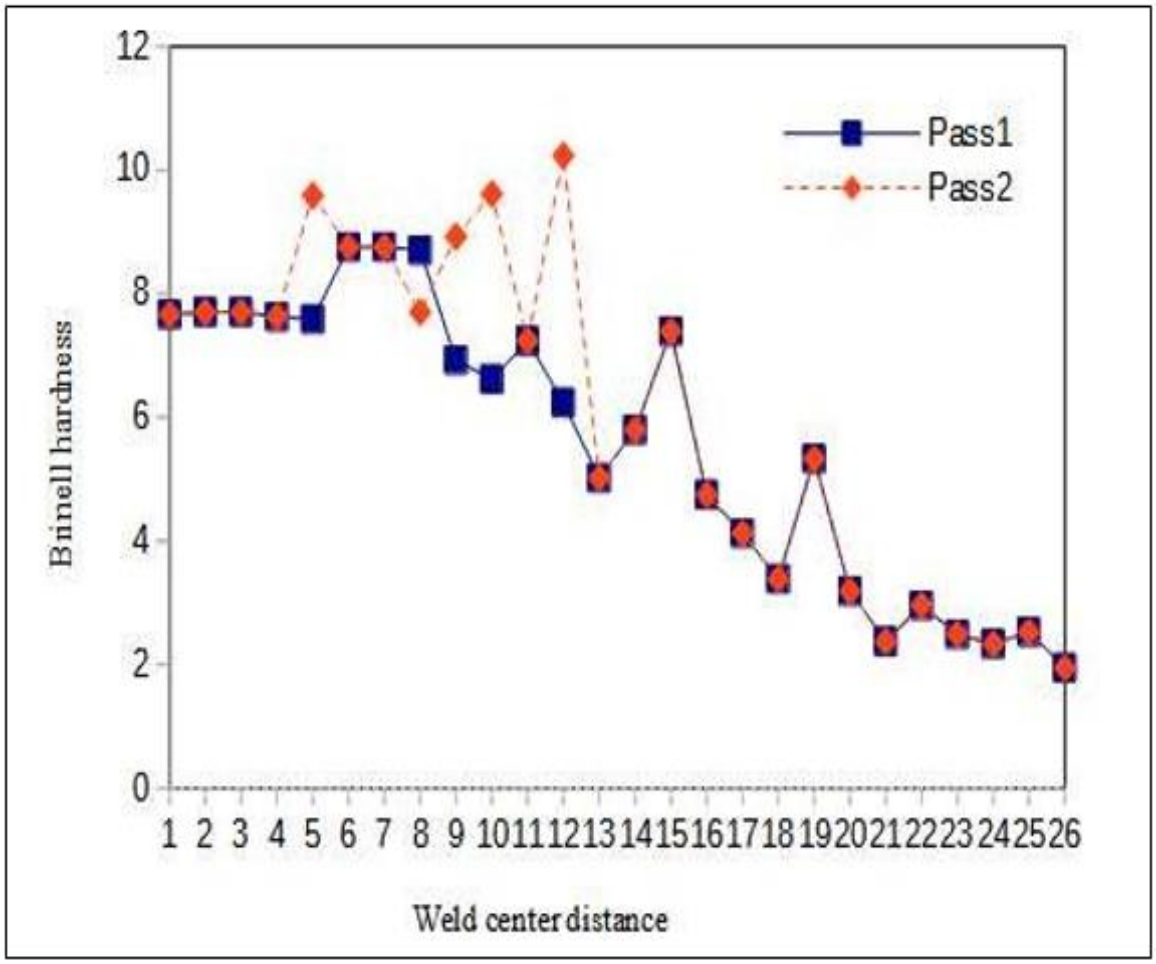


**Figure 12: Hardness variations at the joint interface of AA2024 and AA7075 specimens welded**

Figure 12 presents the hardness distribution along the transition zone of the AA2024 and AA7075 joint, comparing samples welded with single and double FSW passes. In the case of the single-pass weld, the hardness progressively increases from the base metal towards the stir zone on the AA7075 side, peaking at the transition zone's center before gradually decreasing on the AA2024 side, approximately 2mm from the transition region. A similar pattern is observed in the single-pass welded test specimen, where the hardness gradually rises from the base material to the stir zone on the AA7075 side, reaching its highest point at the transition zone and then gradually reducing on the AA2024 side.

**Tianjin Daxue Xuebao (Ziran Kexue yu Gongcheng Jishu Ban)/**
**Journal of Tianjin University Science and Technology**
ISSN (Online):0493-2137
E-Publication: Online Open Access
Vol: 55 Issue: 12:2022
DOI: 10.5281/zenodo.19247821

## 4. CONCLUSION

The study examines the micro structural characteristics of homogeneous and heterogeneous weld joints between aluminum alloys AA2024 and AA7075.

The key conclusions of this research are as follows:

1) The current specimens exhibit a range of micro structural imperfections, including voids and cracks. These defects could be minimized by adjusting the welding speed of the FSW machine.

2) XRD phase analysis identifies the presence of $Al_2Cu$, $Al_2CuMg$, AlCuMg, and $Al_7Cu_2Fe$ constituent granule's in the AA2024 base metal, while $MgZn_2$ and $Al_7Cu_2Fe$ granules are present within the AA7075 base metal.

3) A notable accumulation of Cu-rich particles is detected in the thermally and mechanically influenced region on the advancing side, whereas Zn-enrich granules are mainly concentrated in the retreating side's thermally and mechanically influenced region. This distribution is primarily governed by the compositional differences between the base materials on the AS and RS.

**Nomenclature:**

| | | |
|---|---|---|
| BM | : | Base Material |
| FSW | : | Friction Stir Welding |
| HAZ | : | Heat-Affected Zone |
| TMAZ | : | Thermo-Mechanically Affected Zone |
| NZ | : | Nugget Zone |
| FSP | : | Friction Stir Processing |
| OM | : | Optical Microscopy |
| SEM | : | Scanning Electron Microscopy |
| EDS | : | Energy-Dispersive Spectroscopy |
| XRD | : | X-ray Diffraction |
| AS | : | Advancing side |
| RS | : | Retreating side |
| EBSD | : | Electron Backscatter Diffraction |
| IPF | : | Inverse Pole Figure |

**References**

1) Zhang, Chenghang ; Huang, Guangjie ; Cao, Yu ; Zhu, Yulong ; Huang, Xinde ; Zhou, Yi ; Li, Qilei ; Zeng, Qinghui ; Liu, Qing. (2020). Microstructure evolution of thermo- mechanically affected zone in dissimilar AA2024/7075 joint produced by friction stir welding. *Vacuum, 179*, 109515.

2) Mostafa M. El-Sayed, A.Y. Shash, M. Abd-Rabou, Mahmoud G. ElSherbiny. (2021). Welding and processing of metallic materials by using friction stir technique: A review. *Journal of Advanced Joining Processes, 3*, 100059.

**Tianjin Daxue Xuebao (Ziran Kexue yu Gongcheng Jishu Ban)/**
**Journal of Tianjin University Science and Technology**
ISSN (Online):0493-2137
E-Publication: Online Open Access
Vol: 55 Issue: 12:2022
DOI: 10.5281/zenodo.19247821

3) Zhang, C., Huang, G., Cao, Y., Li, Q., Zhu, Y., Huang, X., & Liu, Q. (2020). Investigation on microstructure and localized corrosion behavior in the stir zone of dissimilar friction-stir-welded AA2024/7075. *Journal of Materials Science*, 15005- 15032. doi:10.1007/s10853-020-05072-w

4) M. Sharifitabar, H. Nami. (2011). Microstructures of dissimilar friction stir welded joints between 2024-T4 aluminum alloy and Al/Mg2Si metal matrix cast composite. *Composites Part B: Engineering, 42*(7), 2004-2012. Retrieved from https://doi.org/10.1016/j.compositesb.2011.05.025.

5) Mishra, R.S. and Ma, Z.Y. (2005). Friction stir welding and processing. *Materials science and engineering: R: reports, 50*(1-2), 1-78.

6) Asim Ahmad Riaz, Ghulam Hussain, Naveed Ullah, Hongyu Wei, Mohammed Alkahtani, Muhammad Naeem Khan. (2021). An investigation on the effects of tool rotational speed and material temper on post-ISF tensile properties of Al2219 alloy. *Journal of Materials Research and Technology, 10*, 853-867. Retrieved from https://doi.org/10.1016/j.jmrt.2020.12.055.

7) Amancio-Filho, S. T., Sheikhi, S., Dos Santos, J. F., &Bolfarini, C. (2008). Preliminary study on the microstructure and mechanical properties of dissimilar friction stir welds in aircraft aluminium alloys 2024-T351 and 6056-T4. *Journal of materials processing technology, 206*(1-3), 132-142.

8) Asadi, P., Besharati Givi, M. K., & Akbari, M. (2016). Simulation of dynamic recrystallization process during friction stir welding of AZ91 magnesium alloy. *The International Journal of Advanced Manufacturing Technology, 83*, 301-311.

9) Coelho, R.S., Kostka, A., Dos Santos, J.F. and Kaysser-Pyzalla, A. (2012). Friction-stir dissimilar welding of aluminium alloy to high strength steels: Mechanical properties and their relation to microstructure. *Materials Science and Engineering: A, 556*, 175- 183.

10) Flores, O.V., Kennedy, C., Murr, L.E., Brown, D., Pappu, S., Nowak, B.M. and McClure, J.C. (n.d.). Microstructural issues in a friction-stir-welded aluminum alloy. *ScriptaMaterialia, 38*(5), 703-708.

11) Fuller, C.B., Mahoney, M.W., Calabrese, M. and Micona, L. (2010). Evolution of microstructure and mechanical properties in naturally aged 7050 and 7075 Al friction stir welds. *Materials Science and Engineering: A, 527*(9), 2233-2240.

12) Iqbal, M. P., Tripathi, A., Jain, R., Mahto, R. P., Pal, S. K., & Mandal, P. (2020). Numerical modelling of microstructure in friction stir welding of aluminium alloys. *International Journal of Mechanical Sciences, 185*, 105882.

13) Kumar, K. S. A., Murigendrappa, S. M., & Kumar, H. (2019). Experimental investigation on effects of varying volume fractions of SiC nanoparticle reinforcement on microstructure and mechanical properties in friction-stir-welded dissimilar joints of AA2024-T351 and AA7075-T651. *Journal of Materials Research, 34*(7), 1229-1247.

14) Liu, P., Shi, Q., Wang, W., Wang, X. and Zhang, Z. (2008). Microstructure and XRD analysis of FSW joints for copper T2/aluminium 5A06 dissimilar materials. *Materials letters, 62*(25), 4106-4108.

15) Ma, Z. Y., Feng, A. H., Chen, D. L., & Shen, J. (2018). Recent advances in friction stir welding/processing of aluminum alloys: microstructural evolution and mechanical properties. *Critical Reviews in Solid State and Materials Sciences, 43*(4), 269-333.

16) Mohammadtaheri, M. (2012). A new metallographic technique for revealing grain boundaries in aluminum alloys. *Metallography, Microstructure, and Analysis, 1*, 224- 226.

17) Nakata, K. (2005). Friction stir welding of copper and copper alloys. *Welding international, 19*(12), 929-933.

**Tianjin Daxue Xuebao (Ziran Kexue yu Gongcheng Jishu Ban)/**
**Journal of Tianjin University Science and Technology**
ISSN (Online):0493-2137
E-Publication: Online Open Access
Vol: 55 Issue: 12:2022
DOI: 10.5281/zenodo.19247821

18) P. Cavaliere, F. Panella. (2008). Effect of tool position on the fatigue properties of dissimilar 2024-7075 sheets joined by friction stir welding. *Journal of Materials Processing Technology, 206* (1-3), 249-255. Retrieved from https://doi.org/10.1016/j.jmatprotec.2007.12.036

19) Rhodes, C. G., Mahoney, M. W., Bingel, W. H., Spurling, R. A., & Bampton, C. C. (1997). Effects of friction stir welding on microstructure of 7075 aluminum. *Scriptamaterialia, 36*(1), 69-75.

20) Sakthivel, T., Sengar, G.S. and Mukhopadhyay, J. (2009). Effect of welding speed on microstructure and mechanical properties of friction-stir-welded aluminum. *The International Journal of Advanced Manufacturing Technology, 43*, 468-473.

21) Silva, A.C.F., De Backer, J. and Bolmsjö, G. (2017). Temperature measurements during friction stir welding. *The International Journal of Advanced Manufacturing Technology, 88*, 2899-2908.

22) Sizova, O., Shlyakhova, G.V., Kolubaev, A., Kolubaev, E.A., Psakhie, S.G., Rudenskii, G., Chernyavsky, A.G. and Lopota, V. (2014). Microstructure features of aluminum alloys welded joint obtained by friction stir welding. *Advanced Materials Research, 872*, 174-179.